The Corrosion Behavior of Chromel and Alumel in the Hydrogen Base Gas Mixture of 80%H2+15%CO+5%CO2 at Elevated Temperatures

Transactions of the Japan Institute of Metals, Vol. 22, No. 5 (1981), pp. 291 to 300

The Corrosion Behavior of Chromel and Alumel in the Hydrogen Base Gas Mixture of 80%H_2+15%CO+5%CO_2 at Elevated Temperatures

By Tatsuo Shikama*, Tatsuhiko Tanabe*, Masakazu Fujitsuka**, Hiroshi Araki*, Heitaro Yoshida*, and Ryoji Watanabe*

The corrosion behavior of Chromel and Alumel was studied in a hydrogen base gas mixture of 80%H_2+15%CO+5%CO_2 at elevated temperatures. The gas simulated that used for the direct reduction of iron ores in the steelmaking process which is now being developed in Japan. Chromel and Alumel were selectively oxidized at elevated temperatures. Chromel was also found to be carburized at about 923 K, where the present gas mixture had the maximum carbon potential and severe carbon deposition (sooting) occurred. These results agreed with those expected from thermodynamic analysis of the present gas mixture.

The severe internal oxidation occurred at about 873–1073 K in Chromel, showing a strong correlation with the free carbon deposition having also occurred in the same temperature range.

The corrosion also affected the magnetic properties of Chromel with changing from paramagnetic to ferromagnetic, whilst Alumel shows an increasing magnetic susceptibility. It is considered that magnetic susceptibility measurements could be a useful non-destructive test for corrosion of Chromel and Alumel.

(Received June 16, 1980)

I. Introduction

Deterioration of the electro-motive force (emf) of thermocouples has been noticed during long-term measurements of temperature in corrosive environments[1][2]. In the course[3] of research on the properties of nickel-base heat resistant superalloys at high temperatures in the hydrogen base gas mixture of 80%H_2+15%CO+5%CO_2, which simulates the reducing gas used in the direct steel making system now being developed in Japan[4], the present authors perceived that the emf of Chromel-Alumel (CA) thermocouples deteriorated drastically.

This deterioration of the emf of CA thermocouples was found to be caused by the corrosion of Chromel and Alumel by the hydrogen base gas mixture at elevated temperatures. The corrosion of Chromel by the selective oxidation of chromium, causing a reduction of the chromium content in the alloy, was particularly evident.

The present study was intended to investigate the corrosion behavior of Chromel and Alumel in the hydrogen base gas mixture, which has a low concentration of oxidizing gases and has a high carbon potential, as this is the first step to improve the stability of the emf of CA thermocouples in those atmospheres. Furthermore, (as Chromel is a Ni-10 wt%Cr alloy) it would be instructive for the understanding of the corrosion behavior of nickel base heat resistant superalloys, most of which contain some amount of chromium as an alloying element for the improvement of their corrosion resistance at high temperatures. In addition to the usual study of corrosion behavior, measurements of magnetic moment (susceptibility) were carried out and were proved to be very useful for evaluating the corrosion rates of Chromel. This technique would be applicable to nickel-base heat resistant superalloys.

* National Research Institute for Metals, Tsukuba Laboratories, 1-2-1, Sengen, Sakura-mura, Niihari-gun (Tsukuba academic city), Ibaraki-ken 305, Japan.

** National Research Institute for Metals, 2-3-12, Nakameguro, Meguro-ku, Tokyo 153, Japan.

II. Experimental Procedures

The chemical composition, microstructure and magnetic susceptibility of a Chromel-Alumel[3] thermocouple were examined after

about 7.2Ms exposure to the hydrogen-base gas mixture at elevated temperatures.

The chemical composition of the Chromel and Alumel are given in Table 1 along with that of the hydrogen-base gas mixture used in the present study. The Chromel-Alumel thermocouple was made by Chino Manufac. Co. Ltd, and the detailed chemical analysis of the present gas mixture was already reported elsewhere[3].

Chromel and Alumel wires 0.5 mm in diameter were cut into 2–3 cm lengths, weighed, and the magnetic susceptibility was determined for each piece at room temperature. The specimen numbers and their configurational positions are depicted in Fig. 1 with the temperature to which they were exposed.

A magnetic field, H, with a gradient of dH/dx is applied to the specimen in a quartz holder, which generates a force, F, on the specimen. The generated force, F, can be related to the mass susceptibility, σ, of the specimen,

Table 1 Chemical composition of Chromel and Alumel (in wt%), with composition of the present gas mixture (in vol%).

	Ni	Cr					
Chromel	90	10					
	Ni	Al	Si	Mn			
Alumel	94	3	1	2			
	H_2	CO	CO_2	CH_4	O_2	N_2	Dew point
Gas mixture	Bal.	14.8	4.8	0.12	n.d.	n.d.	below 253 K

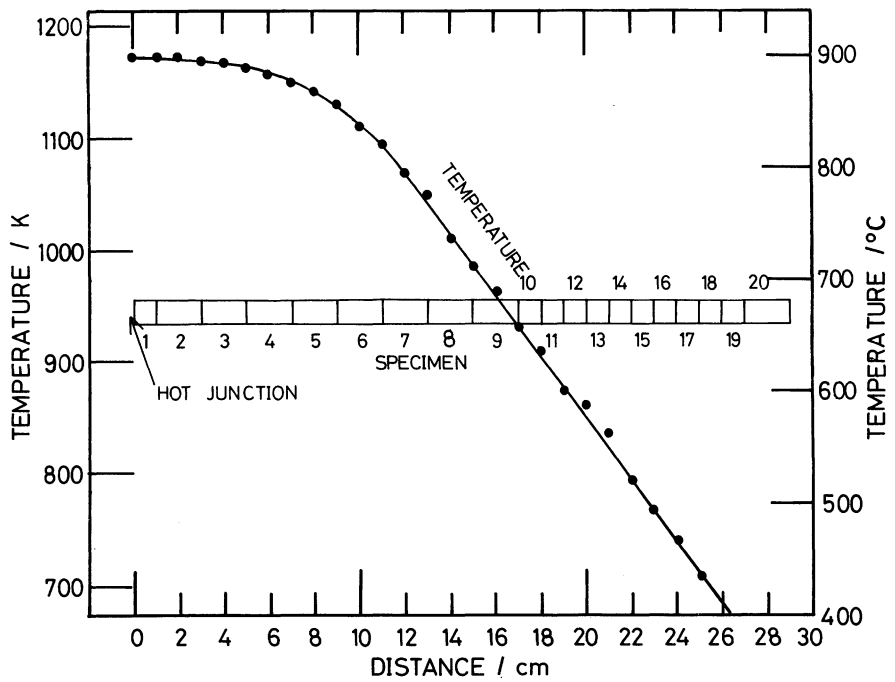

Fig. 1 The specimen configuration and identifying numbers showing the temperature distribution as a function of the distance from the hot junction of the CA thermocouple.

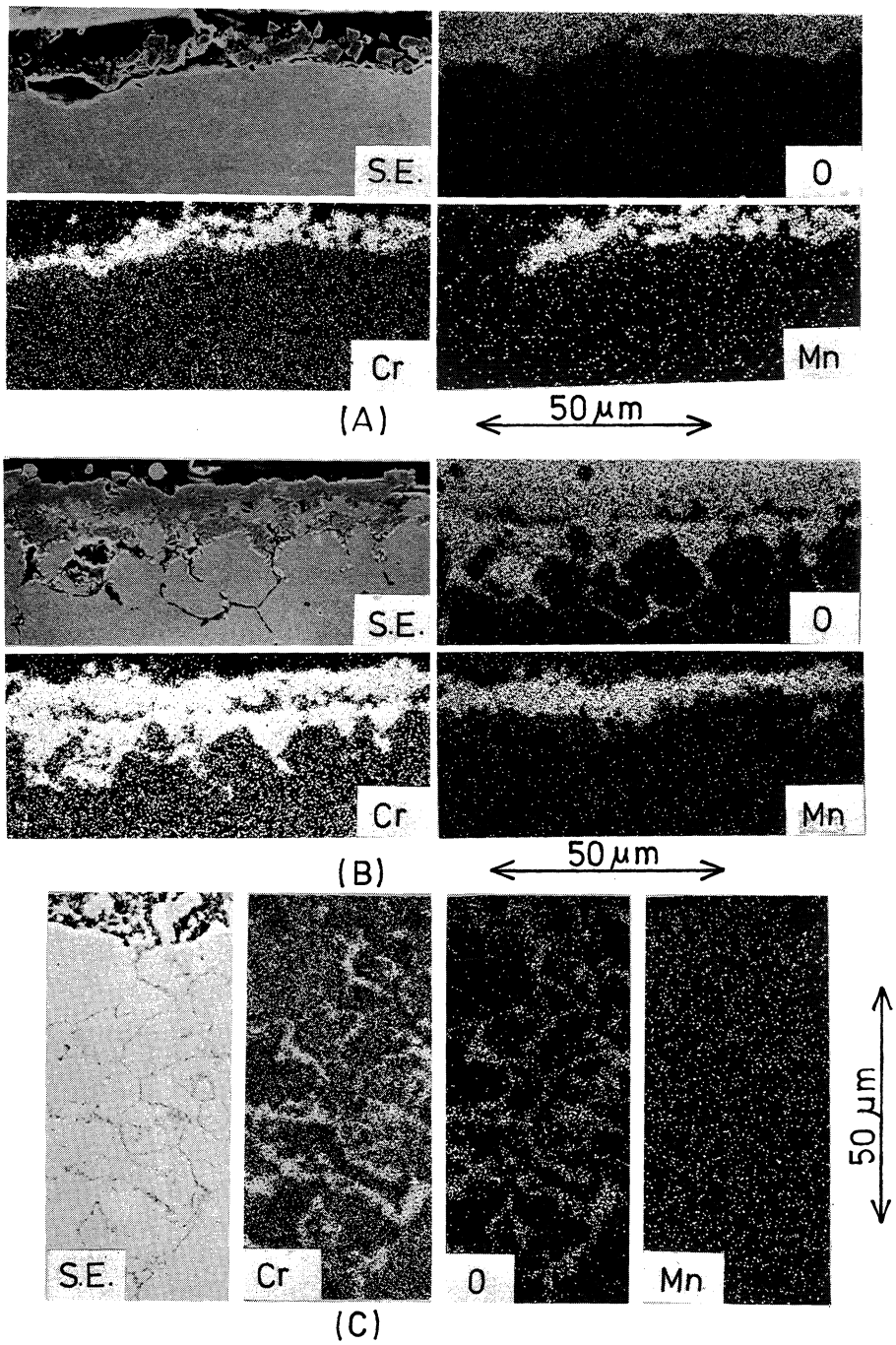

Photo. 1 Characteristic X-ray images (S.E.; Secondary Electron image, O; OK_α image, Cr; CrK_α image, and Mn; MnK_α image) from cross sections of specimens corroded at about 1173 K ((A), specimen No. 1), just below 1173 K ((B), specimen No. 2), and 973 K ((C), specimen No. 9).

whose mass is m, as follows[5],

$$F = M \cdot \mathrm{d}H/\mathrm{d}x, \tag{1}$$

$$M = m\sigma H. \tag{2}$$

The value of $H \cdot \mathrm{d}H/\mathrm{d}x$ was estimated by measuring the force generated on a nickel wire whose susceptibility is well-known.

The surface morphology of the specimen was examined with a scanning electron microscope (SEM). The specimen was then mounted in resin and was lapped with fine alumina particles. After lapping, the specimen was ultrasonically cleaned in ethyl alcohol and was examined in cross section with an optical microscope and an electron probe X-ray micro analyzer (EPMA).

III. Results

Chromel was oxidized in the hydrogen-base gas mixture at elevated temperatures. The surface oxide scale formed at about 1173 K. With decreasing temperature, the corrosion behavior changed from external oxidation to internal oxidation.

The characteristic X-ray images of O, Cr, and Mn are shown in Photo. 1(A), (B), (C), from the cross section of Chromel exposed to the gas mixture at about 1173 K (specimen No. 1), just below 1173 K (specimen No. 2), and 973 K (specimen No. 9), respectively. Chromium was found to be the main oxidized element, and a trace of manganese was contained. The morphology of the internal oxidation layer changed with the temperature as shown in Photo. 2(A)–(E). The internal oxidation proceeded most severely over the temperature range 873–1073 K, and the whole cross section became internally oxidized as shown in Photo. 2(C) and (D).

The internal oxidation of the chromium developed as dispersed particles at higher temperatures as shown in Photo. 2(B) and (C). At lower temperatures, the internal oxidation layer seemed to be finer in morphology than those formed in the higher temperature regions (Photo. 2(C)–(E)).

At about 923 K, the free carbon deposition on the surface of Chromel and the exfoliation of the surface layer was particularly apparent (Photo. 3).

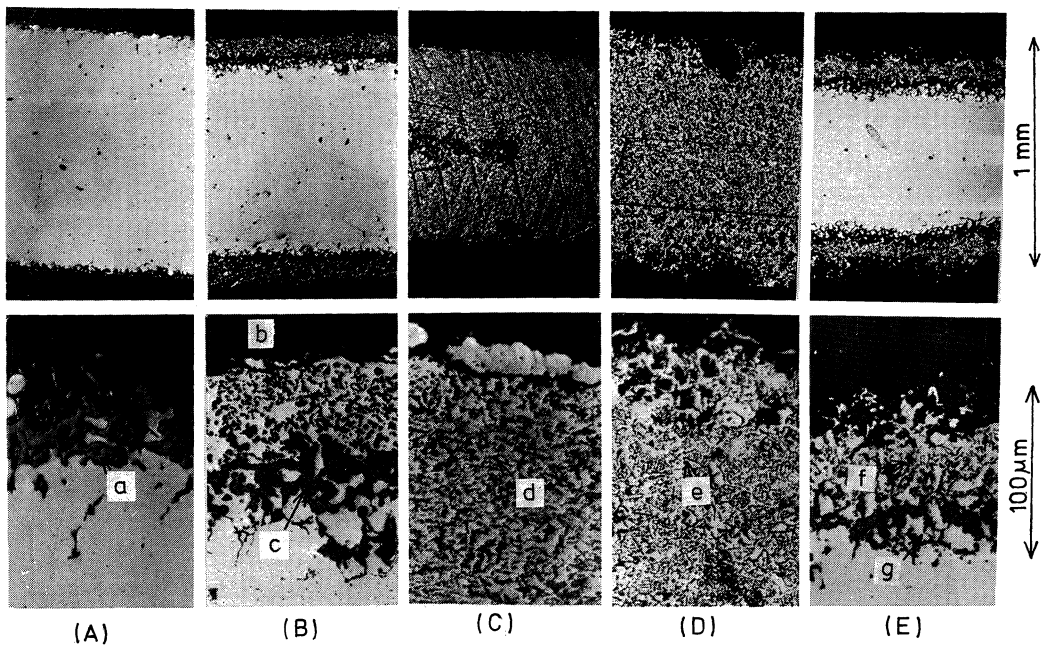

Photo. 2 Microstructures of cross sections of Chromel corroded at just below 1173 K ((A), specimen No. 3), about 1153 K ((B), specimen No. 4), about 973 K ((C), specimen No. 8) and about 923 K ((D), specimen No. 10), and about 873 K ((E), specimen No. 12).

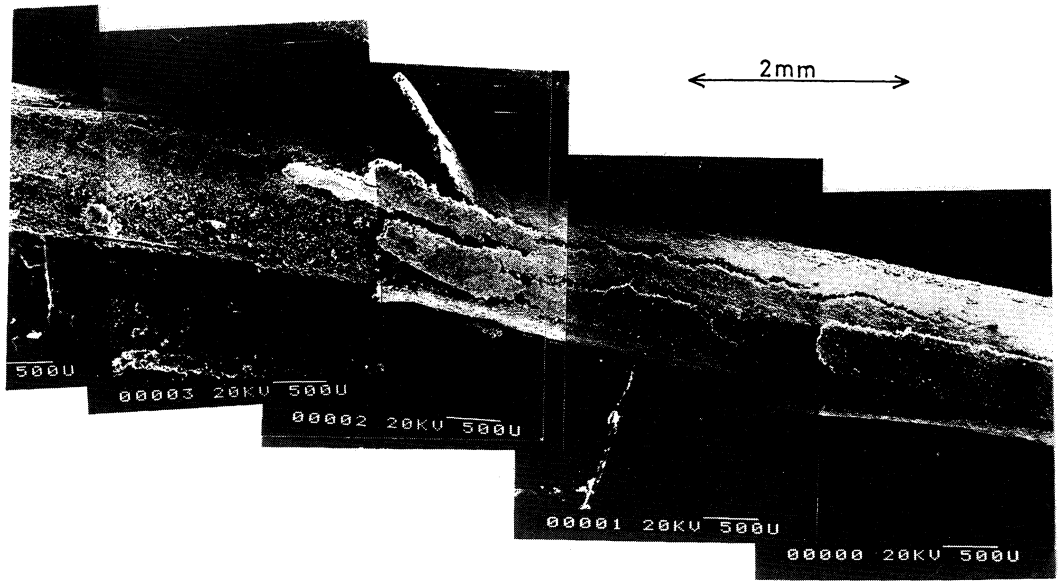

Photo. 3 SEM observation on Chromel corroded at about 923 K.

The EPMA line analysis for C, O, and Cr was conducted in the cross section of the corroded specimens. The results have a good correspondence with the metallographic observations mentioned above. At about 1173 K, a distinct surface oxide scale containing chromium was noticed, while no internal oxidation layer was observed, which can be seen also in Photo. 1(A). Under the surface scale, some diffusion zone, or the depleted zone of chromium was observed. At 1173–1073 K, the internal oxidation layer of chromium extended to the inner region (as shown in Photo. 1(B)) and at about 973 K, most of the cross section changed into the internal oxidation layer (as in Photo. 1(C)). At a temperature of around 923 K, there was some evidence of carburization. (Fig. 2)

The depth of the internal oxidation layer, as obtained from the EPMA line analysis, is plotted as a function of the distance from the hot junction of the thermocouple (Fig. 3).

The intensities of the chromium characteristic X-ray and those of oxygen were obtained at the positions indicated by a-g in Photo. 2(A)–(E). The results and the calculated compositions are tabulated in Table 2. The standard of intensity of the characteristic X-ray of chromium was obtained from pure chro-

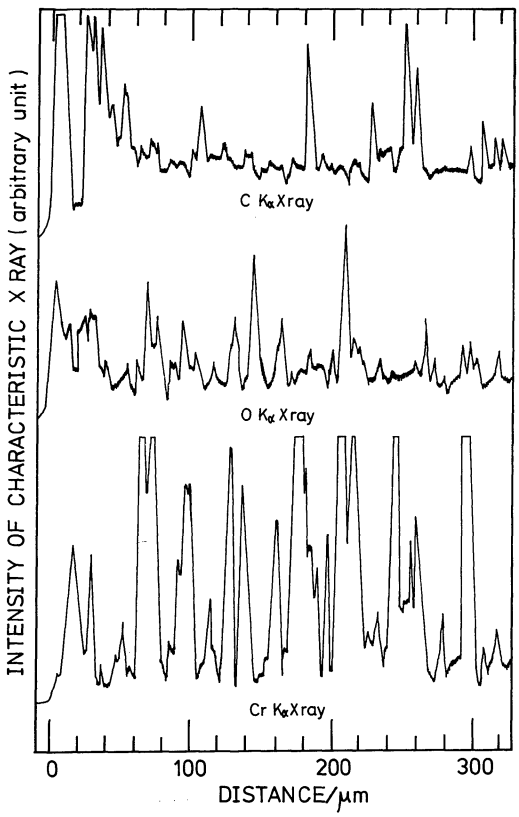

Fig. 2 Intensities of characteristic X-ray of CK_α, OK_α, and CrK_α of specimen No. 10 as a function of distance from the exposed surface. (Chromel corroded at 923 K)

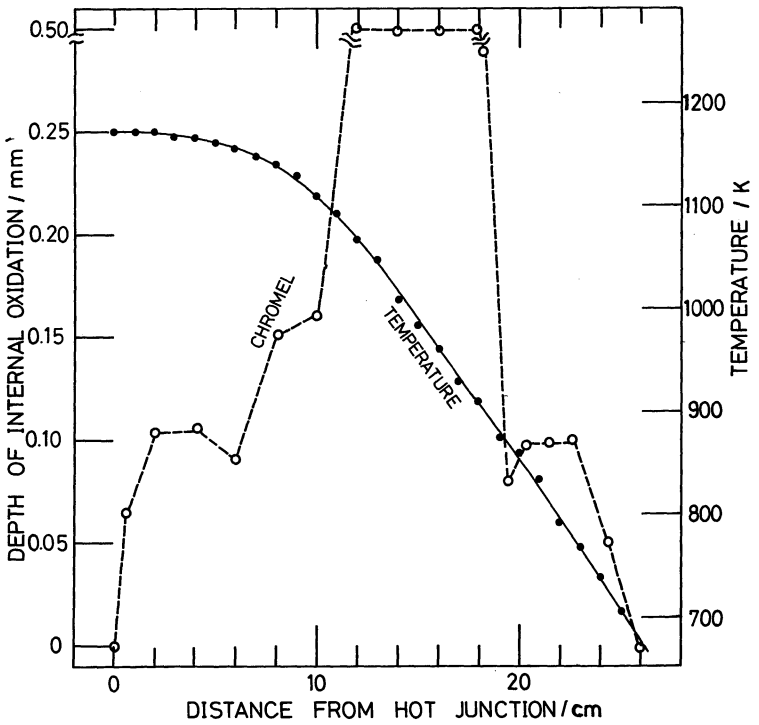

Fig. 3 Depth of internal oxidation in Chromel as a function of distance from the hot junction of the CA thermocouple, obtained by EPMA line analysis.

Table 2 Results of point count of intensities of characteristic X-ray for oxygen and chromium and calculated composition of Cr_2O_x.

Point	Count (Cr)	Count (O)	Count (O)/Count (Cr)	O (wt)/Cr (wt)	O (at)/Cr (at)	Cr_2O_x
(a)	28840	1170	0.041	0.51	1.65	$Cr_2O_{3.3}$
(b)	22760	890	0.040	0.50	1.60	$Cr_2O_{3.2}$
(c)	17910	660	0.037	0.47	1.52	Cr_2O_3
(d)	24300	990	0.040	0.50	1.62	$Cr_2O_{3.2}$
(e)	18240	730	0.040	0.50	1.62	$Cr_2O_{3.2}$
(f)	26790	1090	0.041	0.52	1.68	$Cr_2O_{3.4}$
(g)	17490	710	0.040	0.50	1.62	$Cr_2O_{3.2}$

note; Intensities were counted for ten and five times at each point and averaged. The standard for Cr X-ray was Cr metal and the intensity of Cr X-ray from it was 51800. As for oxygen Al_2O_3 was used and the count was 1180. Points a-g are indicated in Photo. 2(A)~(E).

mium metal, and that of oxygen from Al_2O_3. The correction procedures of Springer[6][8] and Philibert-Duncumb-Shield[7][8] were followed. All the internal oxidation layers examined were shown to have the composition of Cr_2O_3. The chromium concentration in the solid solution of the specimen matrix was also estimated by the same procedure of characteristic X-ray analysis. As for the specimens No. 7–10, the spot size of the electronprobe was too large to exclude any influence of the internal oxide. So it was assumed that the concentration of chromium would be nearly zero, because the whole cross section became internally oxidized as mentioned above.

Alumel was also oxidized internally at high temperatures as shown in Photo. 4, and these oxidation layers were found to consist of oxides of aluminum, manganese and silicon[3]. As the temperature decreased, the depth of

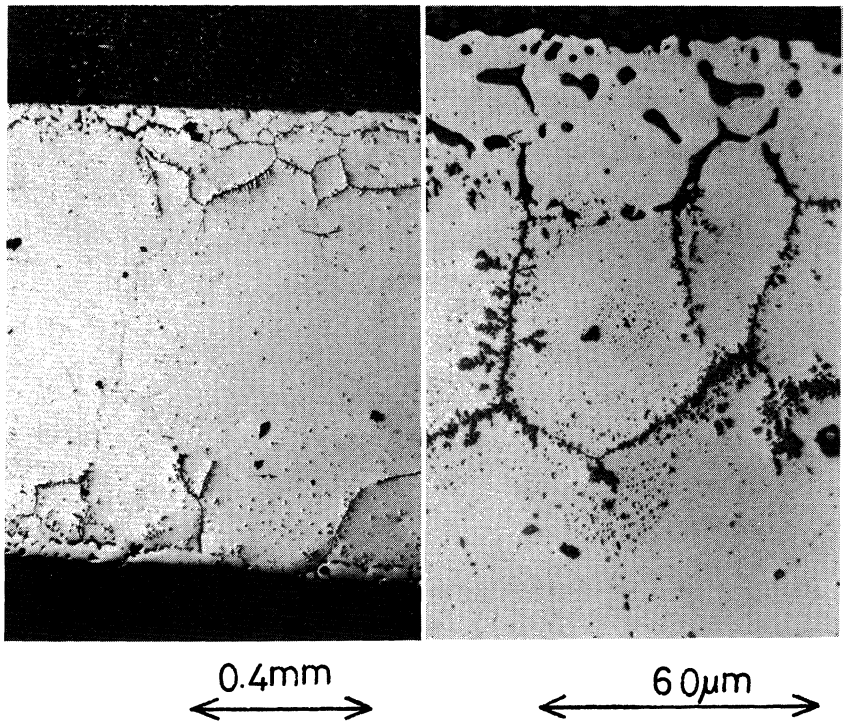

Photo. 4 Microstructure of a cross section of Alumel corroded at about 1173 K.

the internal oxidation decreased and, below 1073 K, a distinct internal oxidation layer was not observed. On the Alumel surface, no free carbon deposition was noticed within the temperature range of room temperature–1173 K with the exception of a small amount of sooting at about 923 K. No exfoliation of the surface layer was noticed.

The force, F, generated in the specimen by the magnetic field, $H \cdot dH/dx$, which would be proportional to the susceptibility of the specimen, is shown as a function of the distance from the hot junction of the thermocouple on Chromel and Alumel in Fig. 4. The force measured was divided by the mass of the specimen used. Before the corrosion, Chromel is paramagnetic and Alumel is ferromagnetic at room temperature. In the case of Chromel, the magnetic susceptibility increased at above 823 K and Chromel changed from paramagnetic to ferromagnetic after exposure to the hot hydrogen-base gas mixture. The susceptibility had a maximum value at 873–973 K. Alumel kept its ferromagnetic property with some increase of magnetic susceptibility at above 773 K.

The susceptibility of nickel-chromium alloys and of nickel-aluminum alloys could be expressed as follows[9][10].

$$M_C(\mu_B)=0.6-0.06C_C, \quad (3)$$

$$M_A(\mu_B)=0.6-0.028C_A, \quad (4)$$

where M_C, and M_A denote the susceptibility of nickel-chromium alloys (containing C_C at% chromium) and of nickel-aluminum alloys (containing C_A at% aluminum), respectively in Bohr magneton units (μ_B). The oxide formed in Chromel was found to be approximately Cr_2O_3 as mentioned above. Cr_2O_3, $MnCr_2O_4$ or aluminum oxide are not ferromagnetic[11]~[13]. Thus, these oxide would not have a large contribution to the magnetic interaction. Therefore, from the eqs. (1)–(4), the chromium aluminum concentrations in the solid solution can be estimated.

The present authors considered that the magnetic measurement could be applied non-destructively. If the mass of the specimen were measured before and after corrosion, one

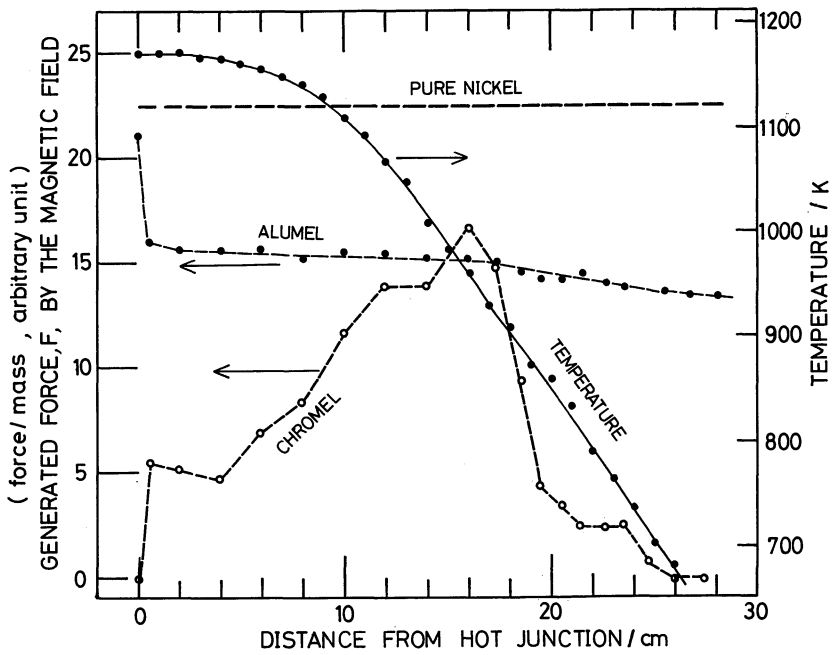

Fig. 4 Force generated in Chromel and Alumel by the magnetic field $H \cdot dH/dx$ as a function of a distance from the hot junction of the CA thermocouple.

could have estimated the actual mass, m, from the mass increase during exposure to the gas mixture, which would exclude the mass of the formed oxide. However, it was not the case of the present study. Also, there are some difficulties to exclude the contribution of the formed oxide from the mass, m, by the metallographic observation in the case of the internally oxidized specimen. Thus the present authors used the total mass as the mass, m, in eq. (2). The estimated chromium concentration is shown in Fig. 5 compared with the results of the EPMA analysis.

IV. Discussion

As has been shown in the previous section, Chromel and Alumel were selectively oxidized, and the oxidation was found to be the cause of the deterioration of the emf of CA thermocouples in the present gas mixture[3]. Chromel, especially, was corroded most severely in the middle range of temperatures of about 873–973 K, in contrast to the corrosion behavior of Alumel where the corrosion proceeded most severely at the highest temperature.

The present gas atmosphere is one of the low oxidizing atmospheres, having a relatively high carburizing potential[3]. Thermodynamic considerations[3][14] showed that nickel was stable and not oxidized, while aluminum, silicon, chromium and manganese were oxidized. Chromium is also expected to be carburized at elevated temperatures. These expectations are consistent with the experimental results.

As for the depth of the internal oxidation, it is expected that the depth will be proportional to $\exp(-A/kT)$. Here, A is a constant, k is Boltzmann's constant and T is the absolute temperature. Hence, the depth of internal oxidation is expected to decrease with decreasing temperature, as is found in the case of the internal oxidation in Alumel.

In the case of Chromel, chromium was externally oxidized and the formation of the protective surface scale was noticed at about 1173 K. Just below 1173 K, however, the surface oxide scale seemed to be not so protective and internal oxidation of chromium occurred. The depth of the internal oxidation increased with decreasing temperature, in contrast to the case of Alumel, and the internal penetration depth of Cr_2O_3 reached its maxi-

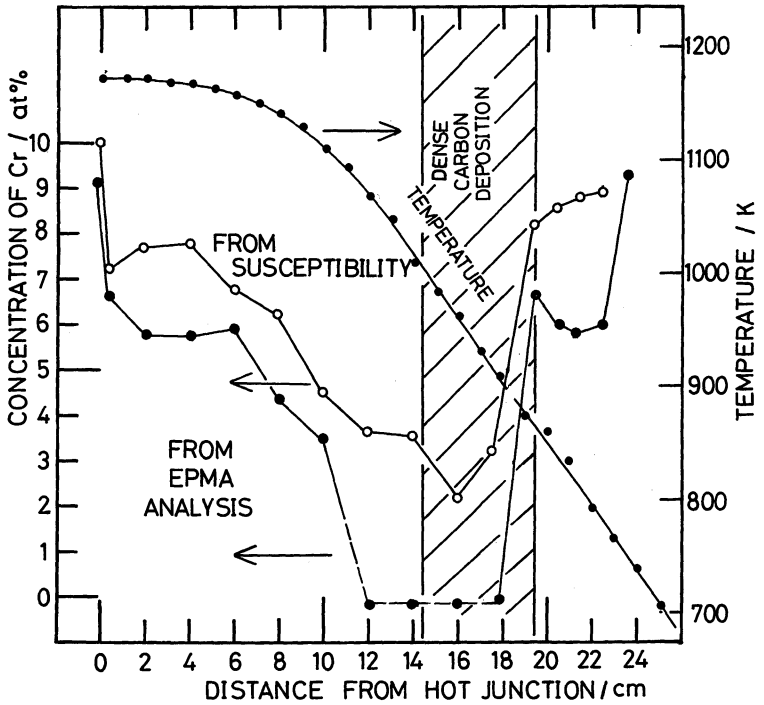

Fig. 5 Calculated concentration of chromium in solid solution in Chromel as a function of distance from the hot junction of the CA thermocouple with temperatures and area of carbon deposition, obtained by the measurement of magnetic susceptibility and by EPMA analysis.

mum value in the temperature range of 873–973 K and decreased with decreasing temperature.

Spooner and Thomas[2] reported that Chromel changed its oxidation form from external to internal over the temperature range of 1273–1323 K in their experiment, where Chromel was corroded for about 172.8 ks whilst being in contact with NiO films in an evacuated quartz tube. In their experiment[2], the internal oxidation layer attained a maximum depth at about 1273 K, just below the transition temperature from external to internal, and the depth of the internal oxidation decreased rapidly with decreasing temperature.

One of the reasons why the present data are different from the above result comes from the fact that in general the atmosphere in this investigation was lower in oxidizing potential than that in their experimental conditions. The main reason would be the present oxidizing potential being changeable with temperature. It will be noticed that the severe internal oxidation and the free carbon deposition (sooting) have a strong correlation with each other as shown in Photo. 3.

It is assumed that the oxidizing potential of the present gas increases over the temperature range in which carbon deposition occurs, probably because the reducing component of the gas will decrease and the oxidizing component of the gas will increase following the carbon deposition. This is the reason why the internal oxidation took place most severely at the temperature range of the carbon deposition. This presumption can also be supported conversely by the fact that Alumel was not oxidized severely over the temperature range, 873–973 K, where the free carbon deposited only slightly on Alumel.

It is not obvious why carbon deposits on Chromel heavily and on Alumel very slightly at about 873–973 K. But it was found in the previous experiment[3][15] that nickel, Cr_2O_3, and $MnCr_2O_4$ had the weakest catalytic effect on free carbon deposition. Chromium also

formed Cr_2O_3 surface scale in the present atmosphere above about 923 K and was found to be a weak catalizer. Chromel, which is in solid solution in the nickel matrix, might play some role in the free carbon deposition as the unoxidized surface would be exposed to the atmosphere through the internal oxidation layer.

It is well known that the nickel base alloys containing more than 10 at% chromium change from paramagnetic to ferromagnetic and are strongly magnetized when they are selectively oxidized or carburized. In the present study, it is recognized that the measurements of the magnetic moment (susceptibility) is a very sensitive method for evaluating the corrosion rates of nickel-chromium alloys qualitatively when one compares Fig. 4 with Fig. 3. The results of the quantitative evaluation of the chromium depletion from the matrix agree well with those obtained by EPMA analysis as shown in Fig. 5.

However, the susceptibility measurements would tend to underestimate the degree of corrosion. This fact would be due to the procedure in which the obtained value of the generated force is divided by mass of the corroded specimen which also contains the mass of the chromium oxide. The agreement would be improved, if the force is divided by the mass excluding the mass of the produced Cr_2O_3.

V. Conclusion

The corrosion behavior of Chromel and Alumel was studied in the hydrogen-base gas mixture of $80\%H_2+15\%CO+5\%CO_2$ at elevated temperatures. Chromel and Alumel were selectively oxidized, which agreed with the thermodynamic predictions of the present gas mixture. Chromel was also carburized at about 923 K. The severe internal oxidation, which occurred at about 873–973 K in Chromel, has a strong correlation with the free carbon deposition which also occurred at about 873–973 K.

The measurement of the magnetic susceptibility of Chromel and Alumel is an easy and appropriate method for evaluating the corrosion rates.

Acknowledgements

The authors are deeply indebted to Dr. M. Uehara for his considerable efforts on the measurements of the magnetic susceptibility. The authors also wish to express their gratitude to Dr. N. Kishimoto and Dr. T. Noda for their frequent, stimulating and helpful discussions. The authors wish to express their special appreciation of the encouraging discussions with Mr. G. P. Pells in AERE Harwell in U.K.

REFERENCES

(1) M. Kohno: Bulletin Japan Inst. Metals, **14** (1975), 881 (in Japanese).
(2) N. F. Spooner and J. M. Thomas: Metal Progress, **68** (1955), 81.
(3) T. Shikama, T. Tanabe, M. Fujitsuka, H. Yoshida and R. Watanabe: Tetsu-to-Hagané, **66** (1980), 418 (in Japanese).
(4) Agency of Industrial Science and Technology, Ministry of International Trade and Industry: *Nuclear Steelmaking Programs in Japan*, Office for National Research and Development Program, Tokyo, (1977).
(5) R. M. Bozorth: *Ferromagnetism*, D. Van Nostrand Company Inc., London, (1951), p. 841.
(6) G. Springer: Fortschr. Miner., **45–1** (1967), 103.
(7) P. Duncumb and P. K. Shields: *The Electron Microprobe*, John Wiley & Sons Co. Ltd. London, (1966), p. 285.
(8) I. Uchiyama, A. Watanabe and S. Kimoto: *X-ray Microanalyzer*, Nikkan Kogyo Shinbunshya, Tokyo, (1972), p. 127.
(9) H. C. Van Elst, B. Lubuch and G. J. Van den Berg: Physica, **28** (1962), 1297.
(10) J. Crangle and J. C. Marian: Phil. Mag., **4** (1959), 1006.
(11) R. S. Tebble and D. J. Craik: *Magnetic Materials*, John Wiley and Sons Co. Ltd., London, (1969), p. 352.
(12) R. M. Moon: Phys. Rev., **136** (1964), A195.
(13) V. J. Folen, G. T. Rado and E. W. Stalder: Phys. Rev. Letters, **6** (1961), 607.
(14) T. Shikama, T. Tanabe, M. Fujitsuka, M. Kitajima, H. Yoshida and R. Watanabe: Met. Trans. AIME, in press.
(15) T. Shikama, T. Tanabe, T. Hirano, M. Fujitsuka, Y. Sakai, H. Araki and H. Yoshida: Z. Metallk., **72** (1981), 30.